Comparisons between integral equation theory and molecular dynamics simulations for realistic models of polyethylene liquids

ARTICLE *in* THE JOURNAL OF CHEMICAL PHYSICS · NOVEMBER 1999

Impact Factor: 2.95 · DOI: 10.1063/1.480335

6 AUTHORS, INCLUDING:

Edmund B. Webb III
Lehigh University
65 PUBLICATIONS **904** CITATIONS

SEE PROFILE

John Mccoy
New Mexico Institute of Mining and Technology
114 PUBLICATIONS **2,055** CITATIONS

SEE PROFILE

Comparisons between integral equation theory and molecular dynamics simulations for realistic models of polyethylene liquids

John G. Curro,[a] Edmund B. Webb III, Gary S. Grest, and Jeffrey D. Weinhold
Sandia National Laboratories, Albuquerque, New Mexico 87185

Mathias Pütz
Center for Microengineered Materials, University of New Mexico, Albuquerque, New Mexico 87106

John D. McCoy
Department of Materials and Metallurgical Engineering, New Mexico Institute of Mining and Technology, Socorro, New Mexico 87185

(Received 20 July 1999; accepted 23 August 1999)

Molecular dynamics (MD) simulations were performed on dense liquids of polyethylene chains of 24 and 66 united atom CH_2 units. A series of models was studied ranging in atomistic detail from coarse-grained, freely-jointed, tangent site chains to realistic, overlapping site models subjected to bond angle restrictions and torsional potentials. These same models were also treated with the self-consistent, polymer reference interaction site model (PRISM) theory. The intramolecular and total structure factors, as well as, the intermolecular radial distribution functions $g(r)$ and direct correlation functions $C(r)$ were obtained from theory and simulation. Angular correlation functions were also obtained from the MD simulations. Comparisons between theory and simulation reveal that PRISM theory works well for computing the intermolecular structure of coarse-grained chain models, but systematically underpredicts the extent of intermolecular packing, and overpredicts the compressibility, as more realistic details are introduced into the model. We found that the PRISM theory could be considerably improved by adding a tail function to $C(r)$ beyond the effective hard core diameter. The range of this tail function was determined by requiring the theory to yield the correct compressibility. The intermolecular radial distribution functions from this modified PRISM theory were in excellent agreement with $g(r)$'s obtained from the simulations. © *1999 American Institute of Physics.* [S0021-9606(99)50843-X]

I. INTRODUCTION

Significant advances have been made in recent years in our ability to realistically model, both theoretically and through computer simulation, amorphous polymers in the condensed phase. It is now possible to perform molecular dynamics[1–4] (MD) and Monte Carlo[5,6] simulations on long chain oligomers in the liquid state using realistic united atom or explicit atom models. Unfortunately, because of computer time requirements, these simulations are still restricted to low degrees of polymerization with the maximum sites per chain of order 100. From a theoretical perspective, integral equation methods, originally developed for monatomic and small molecule liquids, have been extended to polymer melts and alloys in the polymer reference interaction site model[7] (PRISM). An appealing aspect of PRISM theory is that it allows one to use the single chain structure factor, obtained from a single chain computer simulation, to infer the intermolecular packing and properties of the many chain polymer liquid. Since it is, in principle, less computationally intensive to perform a single chain rather than a full multiple chain simulation, this technique should allow one to study larger systems. The mapping of the single chain onto the many chain problem with PRISM theory is, of course, approximate. The purpose of the present study is to assess its accuracy for realistic models by comparing the theory with full, many chain simulations.

In several previous studies, detailed comparisons were made between PRISM theory and computer simulations of melts[8–10] and blends[11,12] of coarse grained polymer models. In the case of the single component polymer liquid of bead–spring model polymers, interacting with repulsive Lennard-Jones interactions, PRISM theory predicted[8] the intermolecular radial distribution function $g(r)$ to be within 10%–15% of the results from the full, many chain MD simulation. Yethiraj and co-workers[9,10] found similar results for melts of freely jointed chains with hard core interactions between sites based on Monte Carlo simulations. Stevenson and co-workers[11] performed MD simulations on athermal blends as a function of composition for bead–spring models of 50 units in which the bead diameter of one component was 20% larger than the other. The agreement between PRISM theory and simulation was about the same as for the one component melt. Interestingly, the error in the theory was somewhat larger for the smaller size component. More recently, Tillman and co-workers[12] performed MD simulations to study the effect of site/site attractions, superimposed on the repulsive Lennard-Jones potential, on the structure of miscible blends of bead–spring models of 50 units. They found that the intermolecular radial distribution functions were not

[a]Author to whom correspondence should be addressed.

appreciably affected by attractive interactions until the phase boundary was approached. On the whole, agreement between intermolecular packing effects predicted by theory and simulation was found to be quite satisfactory for coarse-grained models of polymers at densities typical of liquids. In fact the agreement between PRISM theory and full simulation is comparable to results found by Chandler[13,14] and colleagues for the RISM theory of small, rigid molecules.

It is well known that coarse-grained representations of a polymer are entirely adequate for predicting properties on a length scale associated with the radius of gyration. However, a more realistic polymer model is probably required if one is interested in making predictions of thermodynamic quantities and other nonuniversal properties that are sensitive to the way the polymer chains pack on a monomeric length scale. In this case an realistic model that manifests a more faithful representation of the monomeric geometry is necessary. Unlike the simple bead–spring or freely-jointed coarse-grained models, a realistic model needed to capture local packing effects may require the use of multiple, overlapping sites, constrained bond angles, and torsional potentials.

To test the ability of PRISM theory to model realistic polymers, comparisons were made between PRISM theory and wide angle x-ray scattering experiments on amorphous polyethylene[15,16] and other polyolefins[17,18] above their crystallization temperatures. As is usually the case, comparisons between statistical mechanics theory and experiment are somewhat ambiguous since the interatomic potentials are not known precisely. By adjustment of the effective Barker–Henderson [see Eq. (2.10)] hard core diameter for polyethylene to $d=3.90$ Å, which is equivalent to the Lennard-Jones parameters $\epsilon/k_B=72$ K and $\sigma=4.14$ Å, almost quantitative agreement was found between the theoretical and experimental structure factors. However, this Lennard-Jones sigma parameter is somewhat larger than most of the accepted united atom potentials[19–25] for methylene groups.

In this study we carried out a definitive test of the ability of PRISM theory to model the structure and local packing of real polymers by comparing the predictions of PRISM theory with MD simulations on liquids using a realistic polymer chain model. Unlike laboratory experiments, in MD simulations the interatomic potentials, chain architecture, torsional barriers, and molecular weight are all precisely known. The current work is concerned with polyethylene; in future studies we will examine more complex polyolefins. Here we performed MD simulations on *n*-alkanes having $N=24$ and 66 repeat units. A series of models was studied with varying degrees of realism ranging from the bead–spring model studied earlier[8] to a united atom model with overlapping sites, constrained bond angle and torsional potentials.

We begin with a brief summary of self-consistent PRISM theory and the methods and models used in the MD simulations. The effect of the various degrees of coarse graining on the radial distribution function and structure factor is then examined with both MD simulation and PRISM. The direct correlation functions are also extracted from the simulation and compared with PRISM theory predictions on the same models. Finally, we demonstrate how the predictions from PRISM theory can be significantly improved by forcing the theory to give the correct compressibility.

II. THEORY AND SIMULATION

The PRISM theory[26–28] of Curro and Schweizer is an integral equation approach that is a generalization to polymers of the reference interaction site model or RISM theory of Chandler and Andersen.[29,30] The principal output of the theory is information about the intermolecular packing of the polymer as expressed through the intermolecular radial distribution function defined as

$$\rho_c g_{\alpha\gamma}(r)=\left\langle \sum_{i\neq j=1}^{N_c} \delta(\mathbf{r}_i^{\alpha})\,\delta(\mathbf{r}-\mathbf{r}_j^{\gamma})\right\rangle, \tag{2.1}$$

where N_c is the number of polymer chains, $\rho_c=N_c/V$ is the chain density, and $\mathbf{r}_i^{\alpha}$ is the position vector of a site α on chain i, α and $\gamma(\neq\alpha)$ are interaction sites on different polymer chains. For a united atom model of polyethylene, if we neglect end effects, all sites are approximately equivalent and correspond to CH_2 moieties. Thus only a single correlation function $g(r)=g_{\alpha\gamma}(r)$ is needed to completely characterize the intermolecular packing.

The starting point for PRISM theory is the generalized Ornstein–Zernike equation[31] of Chandler and Andersen[29,30] that relates the intermolecular total correlation function $h(r)=g(r)-1$ to the intramolecular structure factor $\hat{\omega}(k)$. In Fourier transform space this relationship can be written simply as

$$\hat{h}(k)=\hat{\omega}(k)\hat{C}(k)[\hat{\omega}(k)+\rho\hat{h}(k)], \tag{2.2}$$

where the caret denotes Fourier transformation with wave vector k, $\rho=N\rho_c/V$ is the monomer density, N is the number of monomers (or sites) per chain, and $C(r)$ is the direct correlation function.[31] The single chain structure factor is defined as

$$\hat{\omega}(k)=\frac{1}{N}\sum_{i,j}^{N}\left\langle\frac{\sin(kr_{ij})}{kr_{ij}}\right\rangle \tag{2.3}$$

with the summations i,j being taken over all the sites on a single chain.

Equation (2.2) can be viewed as a mapping of the average intramolecular structure, $\omega(r)$ onto the average intermolecular structure described by the radial distribution function $g(r)$. This mapping, however, involves the direct correlation function. We now make use of the fact that at liquidlike densities, the direct correlation function is short range for sites interacting with strongly repulsive and weakly attractive interactions. This suggests that $C(r)$ can be approximated by a Percus–Yevick (PY) closure[31]

$$C(r)\cong g(r)[1-\exp(\beta v(r))], \tag{2.4a}$$

where $v(r)$ is the site/site interaction potential and $\beta=1/k_BT$. For hard sphere potentials the above equation reduces to

$$\begin{aligned} &g(r)=0 \quad \text{for } r<d,\\ &C(r)\cong 0 \quad \text{for } r>d, \end{aligned} \tag{2.4b}$$

where d is the hard core diameter.

For a given intramolecular structure function $\hat{\omega}(k)$, Eqs. (2.3) and (2.4) can be solved numerically for $g(r)$. In general, however, one would expect[7] that the average intramolecular structure $\hat{\omega}(k)$ and intermolecular packing correlations $g(r)$ would be coupled together thereby requiring a self-consistent solution for both functions. A reasonable first approximation[7] for $\hat{\omega}(k)$ can be obtained by invoking Flory's idea[32] that long range excluded volume forces are screened in the melt. Thus the intramolecular structure function $\hat{\omega}(k)$ can be obtained from a separate, single chain calculation or simulation on a model in which long range repulsive interactions are set to zero beyond some cutoff along the chain backbone. The resulting $\hat{\omega}(k)$, when substituted into Eq. (2.3), leads to predictions for the intermolecular radial distribution function $g(r)$. Such a procedure has been carried out for Gaussian,[33] freely-jointed chain,[26–28] and semiflexible chain models,[34] where $\hat{\omega}(k)$ can be found analytically, and from realistic models[15–17] where $\hat{\omega}(k)$ was found from a single chain Monte Carlo simulation.

Use of the Flory ideality hypothesis enforces the correct scaling of the radius of gyration in the melt ($R_g \sim N^{1/2}$) and gives reasonable predictions for $g(r)$. One significant problem with this method, however, is that intramolecular overlap is allowed for pairs of sites beyond the cutoff. This unphysical overlapping of sites has the effect of reducing the effective packing fraction of the liquid, since some of the sites occupy the same volume. Although the packing fraction can be approximately corrected, a more accurate, though computationally more intensive, process entails the self-consistent solution of PRISM theory for both the intra- and intermolecular structure.

In self-consistent PRISM theory[7] one writes the potential energy U of a single chain in a multiple chain liquid as

$$U(R) = U_0(R) + U_E(R) + W(R), \tag{2.5}$$

where R represents the set of coordinates that define the instantaneous polymer conformation, U_0 contains the local bonding constraints, and U_E is the sum of all the repulsive (excluded volume) interactions. The effect of the other chains acting on our given chain is contained in the solvation potential $W(R)$ which depends on the intermolecular packing. $W(R)$ is generally attractive and tends to counterbalance the intramolecular excluded volume interactions in U_E. In fact, the Flory ideality hypothesis essentially assumes that the intramolecular excluded volume and solvation potentials effectively cancel each other out. Chandler and co-workers[35] suggested that the solvation potential be of the form (in Fourier space)

$$\beta \hat{W}(k) = -\rho \hat{C}^2(k) \hat{S}(k), \tag{2.6}$$

where the total structure factor is defined according to

$$\hat{S}(k) = \hat{\omega}(k) + \rho \hat{h}(k). \tag{2.7}$$

The self-consistent calculation proceeds by initially guessing $W(R)$. A single chain Monte Carlo simulation is then carried out using the intramolecular pair interactions in Eq. (2.5) to obtain $\hat{\omega}(k)$. This single chain structure function is then inputted into PRISM theory in Eqs. (2.3) and (2.4) which leads to a new prediction of the solvation potential through Eq. (2.6). This process is iterated until $\hat{\omega}(k)$ does not change within some tolerance at which time we have a self-consistent solution. Self-consistent PRISM calculations have been carried out on freely-jointed chain liquids by a number of researchers.[36–39] Recently Weinhold and collaborators[18] have carried out an ambitious multiple site, self-consistent PRISM calculation on united atom models of polypropylene and polyisobutylene. In the present investigation we will employ this self-consistent PRISM technique to deduce the intra- and intermolecular structure of polyethylenelike chains having 24 and 66 methylene repeat units.

In this work we will employ the full Lennard-Jones potential to describe the interaction between nonbonded sites

$$V(r) = 4\epsilon \left[\left(\frac{\sigma}{r} \right)^{12} - \left(\frac{\sigma}{r} \right)^{6} \right]. \tag{2.8}$$

It is well known that the structure of a liquid at high density, as characterized by $g(r)$, is largely determined by the repulsive interactions. This fact motivates us, following Weeks, Chandler, and Andersen[31,40] (WCA), to decompose Eq. (2.8) into a reference or repulsive part $V_r(r)$,

$$\begin{aligned} V_r(r) &= 4\epsilon \left[\left(\frac{\sigma}{r} \right)^{12} - \left(\frac{\sigma}{r} \right)^{6} + \frac{1}{4} \right], \quad r \leqslant 2^{1/6}\sigma, \\ V_r(r) &= 0, \quad r \geqslant 2^{1/6}\sigma, \end{aligned} \tag{2.9a}$$

and an attractive or perturbative contribution $V_a(r)$,

$$\begin{aligned} V_a(r) &= -\epsilon, \quad r \leqslant 2^{1/6}\sigma, \\ V_a(r) &= 4\epsilon \left[\left(\frac{\sigma}{r} \right)^{12} - \left(\frac{\sigma}{r} \right)^{6} \right], \quad r \geqslant 2^{1/6}\sigma. \end{aligned} \tag{2.9b}$$

The soft repulsive potential can be approximately mapped to a hard sphere potential with an effective hard core diameter d given by the Barker–Henderson relation[31,41]

$$d = \int_0^\infty \{1 - \exp[-\beta V_r(r)]\} dr. \tag{2.10}$$

In our PRISM calculations on polyethylene we employed the soft repulsive potential in Eq. (2.9a), as well as, the hard sphere potential in Eq. (2.10). MD simulations were performed using both the full Lennard-Jones (truncated at 10 Å) and the soft Lennard-Jones repulsive potentials.

MD simulations were carried out on the seven systems described in Table I. The simulations for polyethylene used the potential parameters of Siepmann *et al.*[21–23] As in the earlier studies,[1–4] PE66 and PE24 consisted of overlapping CH_2 sites with the bond length l fixed. The bond angles θ varied in a harmonic potential about a fixed angle θ_b,

$$V_b(\theta) = \frac{k_b}{2} (\theta - \theta_b)^2. \tag{2.11a}$$

The torsional bond angles ϕ were subject to the torsional potential[3,4,20]

$$V_t(\phi) = \sum_i a_i \cos^i(\phi). \tag{2.11b}$$

The parameters associated with the angular potentials are given in Table II. As indicated in Table I, only models PE66

TABLE I. MD models and parameters. Lennard-Jones parameters for nonbonded united atom interactions are $\epsilon/k=46.5$ (113.5) K and $\sigma=3.93$ (3.93) Å for $CH_2(CH_3)$ sites. Cross terms used the Lorentz–Berthelot scaling rule. For the PE24r and tangent site chains all the sites are identical. The hard core diameter d was obtained from Eq. (2.10).

Model	N	l (Å)	Run time (ns)	T (K)	d (Å)	ρ (Å)$^{-3}$	Description
PE66	66	1.54	14	448	3.59	0.032 94	full LJ potential
PE66r	66	1.54	5	448	3.59	0.032 94	repulsive LJ
PE24	24	1.54	6	405	3.61	0.031 23	full LJ potential
PE24r	24	1.54	6.5	405	3.61	0.031 04	repulsive LJ, all CH_2
PE24f	24	1.54	3	405	3.61	0.0123	free rotat., repulsive LJ
Tan24a	24	3.93	3	405	3.58	0.014 00	tangent sites
Tan24b	24	3.93	3	45	3.99	0.014 00	tangent sites

and PE24 used the full Lennard-Jones potential with attractions. All the other models employed the repulsive Lennard-Jones potential from Eq. (2.9a). In one case (PE24f) we turned off both the torsional and bending potentials. In this freely rotating case we also used the repulsive Lennard-Jones potential between sites separated by three bonds in order to prevent unphysical overlap. The final two systems studied (Tan24a and b) were for freely-jointed chains consisting of nonoverlapping tangent sites. Unlike the previous bead–spring models[42] studied earlier by MD simulation, the bond length l was fixed at $l=\sigma=3.93$ Å.

The MD simulations were obtained from constant volume, constant temperature simulations. The velocity rescaling algorithm of Berendsen[43] was employed to control the temperature. The equations of motion were integrated using the velocity Verlet algorithm[44] with a 5 fs time step. The bond lengths were held constant using the RATTLE algorithm.[44]

III. RESULTS

Both self-consistent PRISM calculations and MD simulations were performed on model PE66r and the results for the single chains structure factor $\hat{\omega}(k)$ are plotted in Fig. 1. Amazingly, the self-consistent PRISM $\hat{\omega}(k)$ is virtually identical to the MD simulation result. One would expect good agreement in the high wave vector regime since both the theory and simulation used identical chain parameters and potentials. The low wave vector portion of $\hat{\omega}(k)$, however, would be expected to depend on condensed phase effects and hence the detailed form of the solvation potential. Since the form of the solvation potential used in the self-consistent PRISM calculation in Eq. (2.6) is only approximate, the agreement between theory and full simulation for $\hat{\omega}(k)$ may be fortuitous. Similarly, the $\hat{\omega}(k)$ found from self-consistent PRISM theory for the PE24r model was virtually indistinguishable from the MD simulation. In the case of the tangent bead models Tan24a and Tan24b, the self-consistent PRISM calculation was not performed but instead, the $\hat{\omega}(k)$ from the MD simulation was used as input to PRISM theory.

Figure 2 shows the intermolecular radial distribution function found for the various models from the MD simulations and the corresponding PRISM calculations. All the PRISM calculations shown in this figure used the soft repulsive potential, Eq. (2.9a). MD simulations were performed using both the full Lennard-Jones potential, Eq. (2.8) (PE66 and PE24), as well as, the soft repulsive form of the potential, Eq. (2.9a) (PE66r and PE24r). Virtually identical MD results for $g(r)$ were found in both cases and so only the repulsive results are shown. This is a validation for polymer melts of the idea from atomic liquid theory[31] stating that the structure of the liquid, at high density, is determined predominantly by the repulsive branch of the potential.

From Fig. 2 we can see that for model Tan24b, good agreement exists between theory and simulation for the intermolecular pair correlation function $g(r)$. This was also seen in earlier studies[8] on bead spring models. It should be noted that in this model $k_BT/\epsilon\cong 1(=0.97)$. With the Lennard-Jones parameter for CH_2 sites of $\epsilon/k_B=46.5$ K, model Tan24b corresponds to a much lower temperature (45 K) than is relevant for polyethylene above the melting temperature. For this reason, we also studied model Tan24a at

TABLE II. Angular parameters[a] for all the PE models.

k_b (bending)	124.18	kcal/(mol rad^2)
θ_b	114.0°	
a_0 (torsion)	2.007	kcal/mol
a_1	4.012	
a_2	0.271	
a_3	−6.290	

[a]Reference 20.

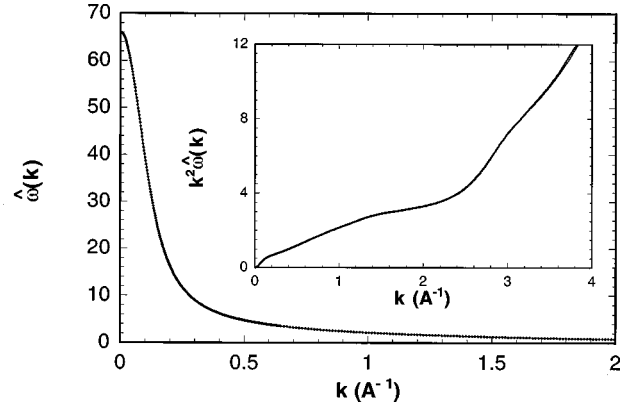

FIG. 1. The intramolecular structure function, defined in Eq. (2.3), as a function of the wave vector k for model PE66r. The points are results from the simulation and the solid curve (underneath points) is from the self-consistent PRISM theory using the repulsive Lennard-Jones potential in Eq. (2.9a). In the inset the results are plotted in Kratky form.

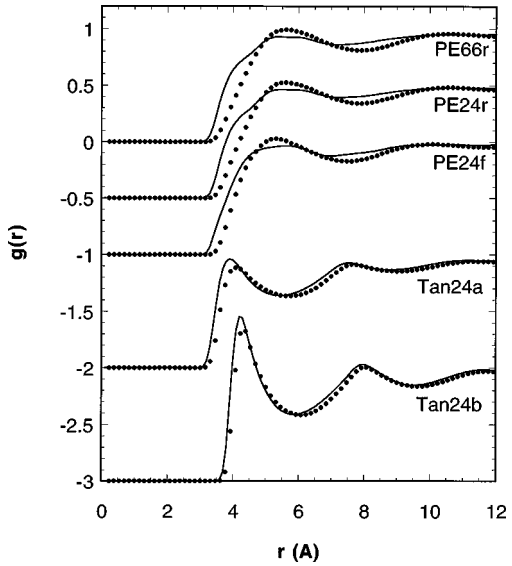

FIG. 2. The intermolecular radial distribution function plotted vs r for the various models. The points were obtained from MD simulations. The solid curves for the PE models were determined from self-consistent PRISM theory using the repulsive Lennard-Jones potential in Eq. (2.9a). The solid curves for the Tan models were obtained from PRISM theory with the MD simulation results for $\hat{\omega}(k)$ as input. The various curves are displaced vertically from each other for the purpose of clarity.

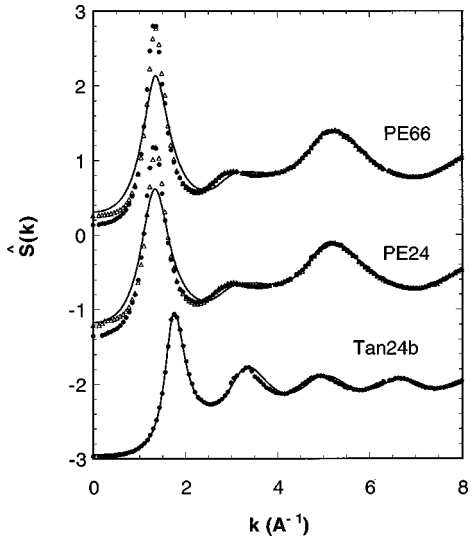

FIG. 3. The total structure factor $\hat{S}(k)$ as a function of wave vector k for the various models indicated. The filled circles are from MD simulations with purely repulsive interactions of Eq. (2.9a). The open triangles are the corresponding MD results using the full Lennard-Jones interactions between sites. The solid curves for the PE models were determined from self-consistent PRISM theory using the repulsive Lennard-Jones potential in Eq. (2.9a). The solid curve for the Tan model was obtained from PRISM theory with the MD simulation results for $\hat{\omega}(k)$ as input. The various models are vertically displaced from each other for the purpose of clarity.

$T=405$ K which corresponds to temperatures more typical of experiments. Note that at the higher temperature, the agreement between theory and experiment is not quite as close as for the lower temperature.

For the more realistic models PE66r and PE24r, it can be seen from Fig. 2 that the agreement between self-consistent PRISM theory and MD simulation is not as good as in the tangent bead models. In particular the theory tends to predict more interpenetration of the repulsive sites than is found in the simulation. Furthermore, the theory predicts less intermolecular structure than simulation since the height and depth of the first peak and valley are underpredicted. Very similar comparisons between PRISM theory and Monte Carlo simulations on united atom models of C_{24} and C_{32} oligomers were found by Dodd and Theodorou.[6] A small improvement in the agreement is seen when the rotational and angular potentials are turned off in model PE24f.

In Fig. 3 we have plotted the total structure factors $\hat{S}(k)$ defined in Eq. (2.7) for various models. Whereas the attractive part of the potential function did not affect $g(r)$, it can be seen in Fig. 3 that attractions significantly affect the structure factor at small wave vectors. This is to be expected since attractions, while not appreciably affecting the structure, are known to have a significant effect on thermodynamic properties. Since the $k\rightarrow 0$ limit corresponds to the thermodynamic limit, it is not surprising that the low wave vector portion of $\hat{S}(k)$ is changed when attractions are turned on. The zero wave vector limit of the structure factor is directly related to the isothermal compressibility $\kappa_T=-(\partial \ln V/\partial P)_T$ through the relation $\hat{S}(0)=\rho k_B T \kappa_T$. In Table III we have tabulated the characteristic ratio from the MD simulations along with the zero wave vector structure factor. Also shown is the corresponding PRISM predictions for $\hat{S}(0)$. Note that PRISM theory consistently predicts a higher compressibility than found from the simulation. In the case of the tangent bead spring model, the PRISM structure factor is in excellent agreement with the simulation. In the realistic models PE66, PE66r, PE24, and PE24r, PRISM theory underpredicts the height of the main peak in the structure factor. Therefore, based on both $g(r)$ and $\hat{S}(k)$, PRISM theory seems to predict a less ordered liquid structure for the realistic models of polyethylene than found from the full MD simulations.

IV. THE DIRECT CORRELATION FUNCTION

From $g(r)$ for the various models in Fig. 2, it is clear that PRISM theory becomes less accurate as we systematically progress in realism from a tangent bead-spring model to a detailed, united atom model of polyethylene. In order to investigate this further we extracted the direct correlation functions from the MD simulation data. From Eqs. (2.2) and (2.7) it can be shown that $\hat{C}(k)$ is related to the intramolecular and total structure factors according to

TABLE III. MD results.

Model	R_g(Å)	C_N[a]	$\hat{S}(0)$	$\hat{S}(0)$(PRISM)
PE66	13.34	6.93	0.2614	
PE66r	13.35	6.94	0.1332	0.3096
PE24	6.75	5.01	0.2872	
PE24r	6.70	4.94	0.1500	0.3263
PE24f	6.92	5.27	0.1173	
Tan24a	9.51	1.84	0.086 44	
Tan24b	9.67	1.53	0.033 95	0.054 09

[a]Column 3 is the characteristic ratio defined as $C_N=6R_g^2/(N-1)l^2$.

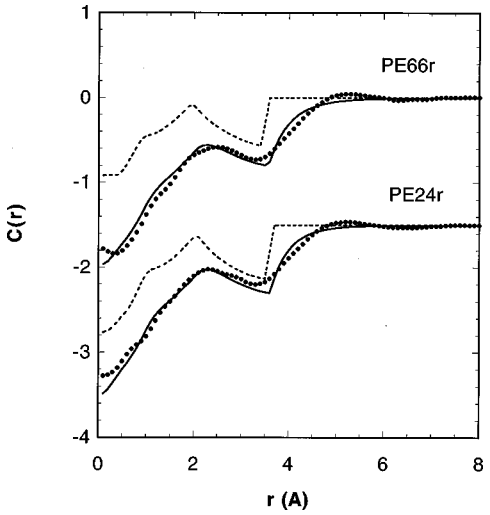

FIG. 4. The direct correlation function plotted vs r for two models indicated. The solid points were extracted from MD simulations from $\hat{\omega}(k)$ and $\hat{S}(k)$ followed by Fourier inversion. The dashed curves were obtained from self-consistent PRISM theory for a hard core potential using hard core diameters d from Table I. The solid curves were obtained from the modified self-consistent PRISM theory discussed in the text. The models are displaced vertically for the purpose of clarity.

$$\rho\hat{C}(k)=\frac{1}{\hat{\omega}(k)}-\frac{1}{\hat{S}(k)}. \tag{4.1}$$

After using the MD simulation results for both $\hat{\omega}(k)$ and $\hat{S}(k)$ in Eq. (4.1), we then inverted the Fourier transform to obtain the direct correlation function in real space. In order to avoid introducing artificial features into $C(r)$ due to numerical errors in $\hat{C}(k)$, the MD data were smoothed in k-space prior to Fourier inversion with fast Fourier transform techniques.

The fundamental assumption in PRISM theory leading to the approximate closure relations in Eqs. (2.4) is that the direct correlation function is a short range function of r. In Fig. 4 we plotted the direct correlation functions for the PE66r and PE24r realistic models (points) along with the theoretical predictions (dashed lines). It can be clearly seen that the $C(r)$ from the MD simulation is a longer range than predicted by PRISM theory. From Eq. (4.1) we can write

$$\hat{S}(0)=\frac{N}{1-\rho N\hat{C}(0)}\cong\frac{-1}{4\pi\rho\int_0^\infty r^2C(r)dr}. \tag{4.2}$$

Thus one consequence of the longer range nature of the direct correlation function is that the isothermal compressibility [or $\hat{S}(0)$] is too large relative to the simulation. This is confirmed in Table III, where it can be seen that the PRISM compressibility is about three times larger than from the MD simulation for these realistic models.

The direct correlation function from the Tan24b model is shown in Fig. 5 along with the corresponding PRISM prediction. As expected based on the agreement between theory and simulation for $g(r)$, the theoretical direct correlation function is in closer agreement with the simulation for the tangent chain models than for the realistic models. It can be

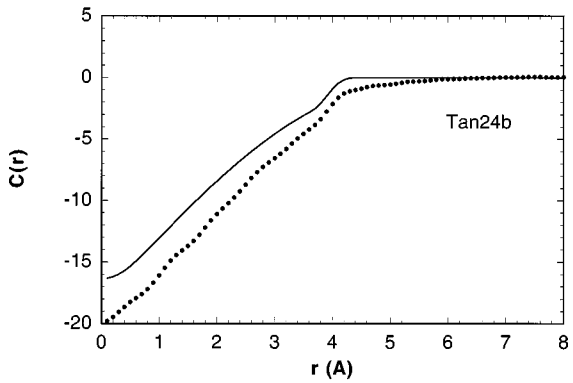

FIG. 5. The direct correlation function for the tangent site chain model as a function of r. The points were extracted from MD simulations from $\hat{\omega}(k)$ and $\hat{S}(k)$ followed by Fourier inversion. The solid curve was obtained from PRISM theory using the repulsive Lennard-Jones potential in Eq. (2.9a). The PRISM calculation used the MD simulation results for $\hat{\omega}(k)$ as input.

seen that even in this case, however, that the PRISM $C(r)$ is shorter range than from the simulation. This leads to the theoretical compressibility being about 1.6 times higher than from the MD simulation as can be seen in Table III.

It appears that an inherent property of PRISM theory using the Percus–Yevick closure is that the compressibility is too large. This suggests that the theory could be improved by forcing the direct correlation function to be longer range. One way of accomplishing this is to simply add a tail function $f(r)$ to $C(r)$ outside the hard core in Eq. (2.4b),

$$\begin{aligned} &g(r)=0 \quad \text{for } r<d, \\ &C(r)\cong f(r) \quad \text{for } r>d. \end{aligned} \tag{4.3}$$

A Yukawa tail function was successfully applied to atomic[45,46] and diatomic liquids[47] where the two Yukawa parameters were chosen to satisfy thermodynamic constraints in the equation-of-state. Yethiraj and Hall[48] used a Yukawa tail function to describe freely-jointed polymer chains. In their case, the two Yukawa parameters were chosen to match the compressibility and the discontinuity in $C(r)$ at the hard core diameter from their tangent hard sphere simulations. Here we adopt a similar idea.

In this work we want to mimic polymers having a continuous potential and direct correlation function using a hard core polymer model. Toward this end, we approximate $f(r)$ to be continuous at the hard core diameter and to have a power law form

$$\begin{aligned} &g(r)=0 \quad \text{for } r<d, \\ &C(r)\cong C_{\mathrm{HC}}(d)\left(\frac{d}{r}\right)^{\lambda} \quad \text{for } r\geqslant d. \end{aligned} \tag{4.4}$$

Thus, we have only one adjustable parameter λ which we determine by matching the isothermal compressibility between theory and simulation (or experiment). The generalized Ornstein–Zernike equation was solved using the above closure together with the same $\hat{\omega}(k)$ input as before. The range of the tail λ was then adjusted until the zero wave vector structure factors agreed with data in Table III. The values of λ required to force concordance with the compress-

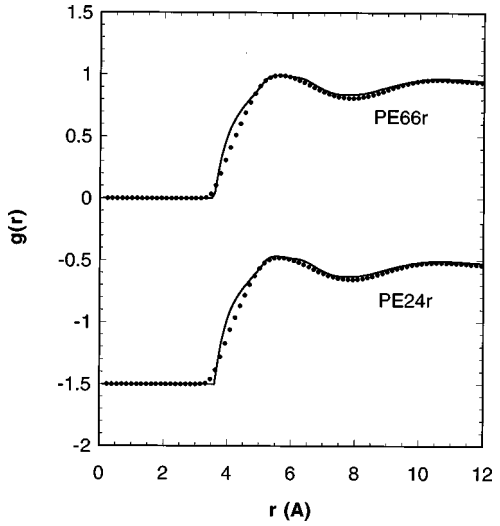

FIG. 6. The intermolecular radial distribution functions plotted vs r for the models indicated. The points are from the MD simulations. The solid curves were obtained from the modified self-consistent PRISM theory discussed in the text. The models are displaced vertically for the purpose of clarity.

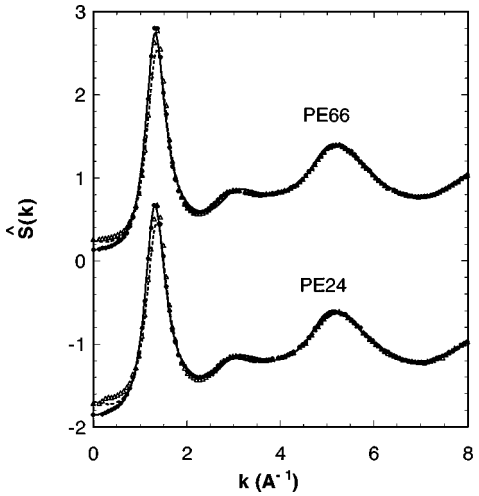

FIG. 7. The total structure factor as a function of wave vector k for the models indicated. The filled circles are from MD simulations with purely repulsive interactions of Eq. (2.9a). The open triangles are the corresponding MD results using the full Lennard-Jones interactions between sites. The solid curves are from the modified self-consistent PRISM theory discussed in the text using the hard core potential. The dashed curves were obtained using the RPA correction for attractive interactions in Eq. (4.7). The models are displaced vertically for the purpose of clarity.

ibility were 7.50 and 8.70 for models PE66r and PE24r, respectively. Of course, a discontinuous Yukawa function or other form of $f(r)$ could be also employed for the tail function, but additional parameters would need to be determined.

The modified PRISM results are given in Fig. 4 as the solid lines; a considerable improvement can be seen in these direct correlation functions. When we now use these $C(r)$ functions to evaluate the intermolecular pair correlation function $g(r)$, much better agreement is seen in Fig. 6 with the MD simulation. Note that $g(r)$ is continuous at $r=d$ as required by the continuity of $C(r)$. It can be observed that the modified theory still predicts slightly more overlap of the sites at about 4 Å. This may be associated with small deviations between the modified $C(r)$ functions and simulation at about 4 Å seen in Fig. 4. This suggests that a minor change in the form of the tail of the direct correlation function may be able to account for the remaining deviations in $g(r)$ between theory and simulation. The modified PRISM theory was also used to obtain the structure factors which are compared in Fig. 7 with the results from MD simulation. Excellent agreement is seen between the modified theory and simulation.

If one is willing to allow the experimental or simulated compressibility to be introduced into the theory, it can be seen that the modified PRISM theory gives a satisfactory description of the structure of polyethylene. Thus one should be able to employ this modified PRISM theory to study higher molecular weight polymer liquids than could be treated with computer simulation. In our case, we employed $\hat{S}(0)$ found in the MD simulations, using the soft repulsive potential of Eq. (2.9a). This was used to fix the range of the tail on $C(r)$ using PRISM theory with the same repulsive potential. As is evident in Fig. 3, attractive interactions have a significant effect on the compressibility and $\hat{S}(0)$. Since experimental data on real polymer systems obviously requires the use of the full potential, with attractions, one either needs to use the full potential with PRISM theory or correct the experimental compressibility for the attractive interactions.

Previous work[8] has demonstrated that PRISM theory works best when applied to purely repulsive interactions. Including attractive interactions in PRISM theory tends to overcompensate for the effect of attractions on the structure of the liquid. Hence, we must correct for the effect of attractions on $\hat{S}(0)$ in order to apply experimental compressibilites for the purposes of adjusting the range of $C(r)$. This correction can be achieved through perturbation theory[31] as was done earlier for polyethylene.[49] A more convenient route for our purposes, however, is through the RPA approximation[31]

$$C(r) \cong C_0(r) - \beta V_a(r), \tag{4.5}$$

where $C_0(r)$ is the direct correlation from the repulsive reference system and $V_a(r)$ is the attractive part of the potential given in Eq. (2.9b). Rearrangement of Eq. (4.1) gives

$$\frac{1}{\hat{S}(k)} = \frac{1}{\hat{\omega}(k)} - \rho \hat{C}(k). \tag{4.6}$$

Substitution of the RPA approximation of Eq. (4.5) into Eq. (4.6) leads to a relation between the structure factors involving the full and repulsive potentials

$$\frac{1}{\hat{S}_0(k)} \cong \frac{1}{\hat{S}(k)} - \rho\beta \hat{V}_a(k), \tag{4.7}$$

where $\hat{S}_0(k)$ is the structure factor for the purely repulsive system. For the WCA decomposition of the Lennard-Jones potential in Eqs. (2.9) $\hat{V}_a(k)$ can be found analytically in the zero wave vector limit. Thus we arrive at the simple relation

$$\frac{1}{\hat{S}_0(0)} \cong \frac{1}{\hat{S}(0)} + \frac{64\pi\beta\epsilon\sigma^3}{9\sqrt{2}}. \tag{4.8}$$

Thus one could apply modified PRISM theory to polymer systems using experimental data for the compressibility together with Eq. (4.8) to adjust the range of the tail on the direct correlation function. Equation (4.7) was used to estimate the effect of attractions on the structure factor as a function of wave vector. This estimate is shown as the dashed line in Fig. 7. It can be seen that the $\hat{S}(0)/\hat{S}_0(0)$ ratio, as well as the complete wave vector dependence of the structure factor for the PE66 model is fairly well accounted for by the RPA approximation.

V. DISCUSSION AND CONCLUSIONS

In this investigation we have demonstrated that PRISM theory can be significantly improved by adding a continuous, power law tail function to the hard core direct correlation function. Although we do not show any results here, a similar strategy can also be applied to the direct correlation function using a model with a soft repulsive potential. Here one can simply adjust the Lennard-Jones parameters to force agreement with the compressibility. Any adjustment of these parameters to increase the apparent size of the sites by making the hard core diameter d larger through Eq. (2.10) will lower $\hat{S}(0)$. This is what was done unintentionally in earlier studies[15,16] comparing PRISM theory with x-ray scattering data on polyethylene where $d=3.90$ was found to give the best agreement.

As mentioned earlier, virtually identical MD results for $g(r)$ were found for the models that used the full Lennard-Jones potential with attractions (PE66, PE24) and the analogous models using repulsive interactions only (PE66r, PE24r). Hence attractive interactions do not appreciably affect the structure of polymer liquids with weakly dispersive interactions at high density. However, for low densities, stronger attractions or lower temperatures, it may be necessary to include the attractive branch of the potential in Eq. (2.9b) in PRISM theory. As found earlier,[7] the PY closure in Eq. (2.4a) does not provide an accurate description of the effect of attractive interactions on the structure of polymer liquids when used in PRISM theory. For this purpose, one could employ the molecular closures of Yethiraj and Schweizer.[7,50] As in the case of the continuous repulsive potential, the direct correlation function could be corrected for the full Lennard-Jones potential, with attractions, by simply adjusting the Lennard-Jones parameters to force the theory to yield the correct compressibility.

We observed that PRISM theory is a good theory for tangent site models with strongly repulsive potentials. Unfortunately, as one applies the theory to polymer models that are more realistic representations of real systems, the accuracy of the theory seems to deteriorate. What aspect of the detailed, united atom model is responsible for the problems in the theory? From Fig. 2 we see that there does not seem to be a single factor, but rather a progression of factors that apparently cause problems in the theory. PRISM theory becomes less accurate each time the model is incrementally moved toward the realistic one. In model Tan24a we see that the theory starts to allow excessive overlap of sites as the effective steepness of the repulsive potential is softened. In model PE24f, we see that allowing the sites to overlap results in a less ordered liquid structure relative to the simulation. Finally, turning on rotational and bond constraints results in further underprediction of the structure.

Another effect to be considered is the possible existence of local angular correlations between nearby polymer chain backbones. PRISM theory assumes that sites interact with spherically symmetric, pairwise additive potentials. In addition, preaveraging the single chain structure factors over all angles would seem to rule out any preferred local orientation effects in the theory. To see if angular correlations were present, we evaluated the angular correlation function from the simulations in a manner similar to Smith and Yoon.[1] Vectors, denoted as **b**, between sites spaced at various lengths along a single chain backbone were constructed. Orientational correlations between these vectors on different chain backbones were then investigated through the correlation function

$$P(r)=\tfrac{1}{2}\left[3\langle\cos^2\theta(r)\rangle-1\right], \tag{5.1}$$

where $\theta(r)$ is the angle between b vectors on different chains and r is the distance between the centers of the vectors. To assess the extent of angular order, we then multiply $P(r)$ by a pair correlation function $g_b(r)$, not between sites, but between the centers of the bond vectors. In addition we examined the size over which angular correlations are important by allowing the b vectors to encompass larger portions of the backbone. For example, for $b=2$, vectors are drawn between sites 1 and 3 along the backbone and involve 2 covalent bonds; for $b=4$ vectors are instead drawn between sites 1 and 5 along the backbone and consist of four covalent bonds.

The angular correlation functions from the MD simulations are plotted in Fig. 8 for various values of b for both the

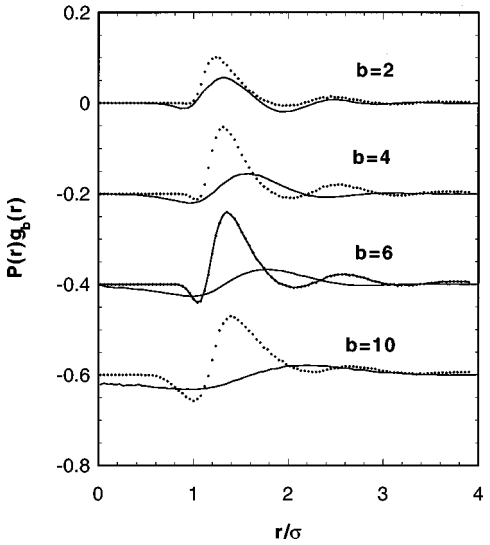

FIG. 8. The angular correlation function $P(r)$ [Eq. (5.1)] times the pair correlation function for bonds $g_b(r)$ as a function of the dimensionless distance r/σ. The filled circles were from MD simulations on model PE24r. The solid curves are from MD simulations on model Tan24b. Results are shown for various values of the b vectors used to determine the angular correlation function as discussed in the text. The data are shifted vertically for the purpose of clarity.

PE66r and Tan24b models. It can be seen that significant angular correlations exist for the realistic chain on distances of one to two site diameters. The corresponding angular correlations for the tangent bead–spring model are substantially less. Furthermore, the angular correlations in the realistic model persist for long distances along the chain backbone out to at least $b=10$. This reflects the larger persistance length, or characteristic ratio, of the realistic model. The existence of large angular correlations may, in part, be related to the high degree of symmetry, and the ability to crystallize, of the polyethylene molecule. One might speculate that angular correlations might be less pronounced in polyolefin chains having a more complex architecture. More complex polyolefins and agreement with PRISM theory will be the subject of a future investigation.

The modification to PRISM theory employed here leads to a significant improvement in predictions of the melt structure of polyethylene and should be applicable to other polymer systems as well. Since the modification necessitates the use of experimental compressibility data, the theory is not complete. We anticipate that a more accurate and complete theory of polymer liquids would result from the application of the density functional theory of Donley, Curro, and McCoy[51] (DCM). In this approach, the pair correlation function can be written as a two-chain average,

$$g(r)=\left\langle \exp\left[\sum_{\alpha\gamma} \beta v_{\alpha\gamma}(r)+\beta W_{\alpha\gamma}(r)\right]\right\rangle, \tag{5.2}$$

where the angular brackets denote the average of a site α on one chain and a site γ on a second chain over all configurations of the pair of chains. $W_{\alpha\gamma}(r)$ is a medium induced potential of the form in Eq. (2.6). Since the evaluation of this solvation potential assumes a knowledge of $g(r)$, the analysis requires a self-consistent solution of Eq. (5.2). A reasonable approximation, however, would simply be to use the PRISM $g(r)$ to compute $W_{\alpha\gamma}(r)$ in the exponent in Eq. (5.2). Then $g(r)$ could be found from a single Monte Carlo simulation involving two chains. The DCM theory would, in principle, include the effects of angular correlations. Furthermore, it should more accurately be able to model overlapping sites since they are explicitly in the simulation.

ACKNOWLEDGMENT

Sandia is a multiprogram laboratory operated by Sandia Corporation, a Lockheed Martin Company, for the U.S. Department of Energy under Contract No. DE-AC04-94AL85000.

[1] G. D. Smith and D. Y. Yoon, J. Chem. Phys. **100**, 649 (1994).
[2] G. D. Smith, W. Paul, D. Y. Yoon, A. Zirkel, J. Hendricks, D. Richter, and H. Schober, J. Chem. Phys. **107**, 4751 (1998).
[3] J. K. Maranas, M. Mondello, G. Grest, S. K. Kumar, P. G. Debenedetti, and W. W. Graessley, Macromolecules **31**, 6991 (1998); **31**, 6998 (1998).
[4] M. Mondello, G. S. Grest, E. B. Webb III, and P. Peczak, J. Chem. Phys. **109**, 798 (1998).
[5] A. Yethiraj, J. Chem. Phys. **102**, 6874 (1995).
[6] For a review see, L. R. Dodd and D. N. Theodoru, Adv. Polym. Sci. **116**, 249 (1994).
[7] For reviews see, K. S. Schweizer and J. G. Curro, Adv. Polym. Sci. **116**, 321 (1994); Adv. Chem. Phys. **98**, 1 (1997).
[8] J. G. Curro, K. S. Schweizer, G. S. Grest, and K. Kremer, J. Chem. Phys. **91**, 1357 (1989).
[9] A. Yethiraj, C. K. Hall, and K. G. Honnell, J. Chem. Phys. **93**, 4453 (1990).
[10] A. Yethiraj and C. K. Hall, J. Chem. Phys. **96**, 797 (1992).
[11] C. S. Stevenson, J. D. McCoy, S. J. Plimpton, and J. G. Curro, J. Chem. Phys. **103**, 1200 (1995); C. S. Stevenson, J. G. Curro, J. D. McCoy, and S. J. Plimpton, *ibid.* **103**, 1208 (1995).
[12] P. A. Tillman, D. R. Rottach, J. D. McCoy, S. J. Plimpton, and J. G. Curro, J. Chem. Phys. **107**, 4024 (1997); **109**, 806 (1998).
[13] D. Chandler, C. S. Hsu, and W. B. Streett, J. Chem. Phys. **66**, 5231 (1977).
[14] C. S. Hsu and D. Chandler, Mol. Phys. **36**, 215 (1978); **36**, 215 (1978).
[15] K. G. Honnell, J. D. McCoy, J. G. Curro, K. S. Schweizer, A. Narten, and A. Habenschuss, J. Chem. Phys. **94**, 4659 (1991).
[16] A. Narten, A. Habenschuss, K. G. Honnell, J. D. McCoy, J. G. Curro, and K. S. Schweizer, J. Chem. Soc., Faraday Trans. **88**, 1791 (1992).
[17] J. G. Curro, J. D. Weinhold, J. J. Rajasekaran, A. Habenschuss, J. D. Londono, and J. D. Honeycutt, Macromolecules **30**, 6264 (1997).
[18] J. D. Weinhold, J. G. Curro, A. Habenschuss, and J. D. Londono, Macromolecules (in press).
[19] J. P. Ryckaert and A. Bellemans, Faraday Discuss. Chem. Soc. **66**, 95 (1978).
[20] W. L. Jorgensen, J. D. Madura, and C. J. Swenson, J. Am. Chem. Soc. **106**, 6638 (1984).
[21] J. I. Siepmann, S. Karaborni, and B. Smit, Nature (London) **365**, 330 (1993).
[22] J. I. Siepmann, M. G. Martin, C. J. Mundy, and M. L. Klein, Mol. Phys. **90**, 687 (1997).
[23] M. G. Martin and J. I. Siepmann, J. Phys. Chem. B **102**, 2569 (1998).
[24] S. K. Nath, F. A. Escobebo, and J. J. de Pablo, J. Chem. Phys. **108**, 9905 (1998).
[25] J. D. McCoy and J. G. Curro, Macromolecules **31**, 9362 (1998).
[26] J. G. Curro, and K. S. Schweizer, Macromolecules **20**, 1928 (1987); J. D. McCoy, S. Mateas, M. Zorlu, and J. G. Curro, J. Chem. Phys. **102**, 8635 (1995).
[27] J. G. Curro and K. S. Schweizer, J. Chem. Phys. **87**, 1842 (1987).
[28] K. S. Schweizer and J. G. Curro, Phys. Rev. Lett. **58**, 246 (1987).
[29] D. Chandler and H. C. Andersen, J. Chem. Phys. **57**, 1930 (1972).
[30] D. Chandler, in *Studies in Statistical Mechanics VIII*, edited by E. W. Montroll and J. L Lebowitz (North-Holland, Amsterdam, 1982), p. 274.
[31] J. P. Hansen and I. R. McDonald, *Theory of Simple Liquids*, 2nd ed. (Academic, London, 1986).
[32] P. J. Flory, J. Chem. Phys. **17**, 203 (1949).
[33] K. S. Schweizer and J. G. Curro, Macromolecules **21**, 3070 (1988); **21**, 3082 (1988).
[34] K. G. Honnell, J. G. Curro, and K. S. Schweizer, Macromolecules **23**, 3496 (1990).
[35] D. Chandler, Y. Singh, and D. M. Richardson, J. Chem. Phys. **81**, 1975 (1984).
[36] K. S. Schweizer, K. G. Honnell, and J. G. Curro, J. Chem. Phys. **96**, 3211 (1992).
[37] A. Yethiraj and K. S. Schweizer, J. Chem. Phys. **97**, 1455 (1992).
[38] J. Melenkevitz, J. G. Curro, and K. S. Schweizer, J. Chem. Phys. **99**, 5571 (1993).
[39] C. Grayce and K. S. Schweizer, Macromolecules **28**, 7461 (1995).
[40] J. D. Weeks, D. Chandler, and H. C. Andersen, J. Chem. Phys. **54**, 5237 (1971).
[41] J. A. Barker and D. Henderson, J. Chem. Phys. **47**, 4714 (1967); Annu. Rev. Phys. Chem. **23**, 439 (1972); Rev. Mod. Phys. **48**, 587 (1976).
[42] G. Grest and K. Kremer, J. Chem. Phys. **92**, 5057 (1990).
[43] H. J. C. Berendsen *et al.*, J. Chem. Phys. **81**, 3684 (1984).
[44] M. P. Allen and D. J. Tildesley, *Computer Simulation of Liquids* (Clarendon, Oxford, 1987).
[45] E. Waisman, Mol. Phys. **25**, 45 (1973).
[46] J. S. Hoye, J. L. Lebowitz, and G. Stell, J. Chem. Phys. **61**, 3253 (1974).
[47] P. T. Cummings, G. P. Morriss, and G. Stell, Mol. Phys. **51**, 289 (1984).
[48] A. Yethiraj and C. K. Hall, J. Chem. Phys. **93**, 5315 (1990).
[49] J. G. Curro, A. Yetharij, K. S. Schweizer, J. D. McCoy, and K. G. Honnell, Macromolecules **26**, 2655 (1993).
[50] A. Yethiraj and K. S. Schweizer, J. Chem. Phys. **97**, 5927 (1992); **98**, 9080 (1993); K. S. Schweizer and A. Yethiraj, *ibid.* **98**, 9053 (1993).
[51] J. P. Donley, J. G. Curro, and J. D. McCoy, J. Chem. Phys. **101**, 3205 (1994).